SEISMIC PERFORMANCE AND FUNCTIONAL INTEGRITY OF AL-SHARQIYAH EXPRESSWAY TUNNEL-2: A FRAMEWORK FOR RESILIENT TUNNEL DESIGN IN OMAN

ABDULLAH ANSARI[1], ISSA EL-HUSSAIN[1], AHMED DEIF[1], ADEL M. E. MOHAMED[1], YOUSUF AL-SHIJBI[1], KHALIFA AL-JABRI[2], GHAZI ALI AL-RAWAS[2] & ZHONGKAI HUANG[3]
[1]Earthquake Monitoring Center, Sultan Qaboos University, Oman
[2]Department of Civil and Architectural Engineering, Sultan Qaboos University, Oman
[3]Department of Geotechnical Engineering, College of Civil Engineering, Tongji University, China

ABSTRACT

This study employed analytical methods based on S-wave propagation to evaluate the seismic performance of the Al-Sharqiyah Expressway Tunnel-2, yielding fragility curves for varying damage levels and seismic loss and functionality over different lifespans. The findings indicate that return periods significantly impact damage probabilities and underscore the need for targeted reinforcement and proactive maintenance to preserve functionality. Recommendations include developing tailored seismic design guidelines, implementing routine monitoring protocols and adopting probabilistic design standards to ensure operational integrity. By integrating these approaches, this study serves as a foundational reference for the sustainable design of tunnels and underground structures in Oman and promoting resilience within the country's transportation infrastructure.

Keywords: seismic, tunnelling, resilience, Al-Sharqiyah, Oman, lifespan.

1 INTRODUCTION

In the Sultanate of Oman, the development of transportation infrastructure indicates a bright outlook, emphasizing a strategic approach to tackling the region's challenging geographical features while improving urban expansion. The government's initiatives over the past decade have yielded significant advancements, with projects of critical national importance aimed at fostering innovation and infrastructure development for societal progress. Among these efforts, the Al-Sharqiyah Expressway stands out as a key transportation project, spanning 191 km and enhancing connectivity between Bidbid and Sur (Fig. 1). This initiative showcases engineering excellence, featuring two tunnels with a combined length of 2,100 m. The first tunnel, Al-Sharqiyah Expressway Tunnel-1 (AST1), is located in Nadab, measuring 650 m, while the second, Al-Sharqiyah Expressway Tunnel-2 (AST2), extends 1,450 m through the mountainous region of Wadi Al-Aqq.

Oman's seismicity is characterized by moderate activity, influenced by tectonic movements along the boundary between the Arabian and Eurasian plates [1]. The fault patterns in the Zagros Mountains significantly affect local seismic behaviour, highlighting the need for robust earthquake-resistant infrastructure. Understanding the seismic response of tunnels is crucial for enhancing earthquake resilience, as it informs design strategies that mitigate damage and ensure structural integrity during seismic events [2]. In this study, an analytical method based on S-wave propagation is employed to evaluate the seismic performance of AST2. The analysis yielded fragility curves for varying damage levels, including minor, moderate, and extensive cases. Additionally, seismic loss and functionality curves are developed for different lifespans (T = 0, T = 50, T = 75 and T = 100 years) across various return periods (RP = 1,000, RP = 750, RP = 500 and RP = 250 years). Considering

www.witpress.com, ISSN 1743-3509 (on-line)
doi:10.2495/ERES250081

Figure 1: Location of Al-Sharqiyah Expressway Tunnel-2 (AST2), Sultanate of Oman.

the overall seismic response of this tunnel, design guidelines and retrofitting strategies are recommended. This study serves as a foundational reference for sustainable tunnel and underground structure design in the Sultanate of Oman, aligning with the United Nations' Sustainable Development Goal 9.

2 SEISMIC ANALYSIS AND PERFORMANCE

The seismic performance of tunnels is influenced by a combination of factors, including the seismic environment, tunnel design, and the specific geological, geotechnical, and geophysical conditions of the region. Building on the foundational closed-form solutions introduced by St John and Zahrah [3] numerous researchers have explored seismic design challenges associated with underground structures. Analytical methods that incorporate P-wave theory [4] and S-wave propagation [5]–[8] have been employed to enhance the understanding of tunnel seismic behaviour. This study utilized the methodologies established by the seismic analyses in Wang [5] and Park et al. [7] (Table 1), assessing the performance of various sections of the Al-Sharqiyah Expressway Tunnel-2 (AST2).

The seismic analysis of Tunnel AST2, as presented in Table 2, revealed significant variations in maximum thrust and bending moments across different sections. The values derived from Wang [5] and Park et al. [7] showed consistent trends. For section AST2A, the maximum thrust decreased by approximately 28%, and the bending moment reduced by about 22% between the two chainages. In section AST2B, a notable drop of around 14% in thrust and 22% in bending moment occurred between 2B.1 and 2B.2, followed by an increase in thrust by 81% and bending moment by 45% in 2B.3. Section AST2C experienced the maximum forces, where the thrust in Wang's model is 10% greater than in Park et al.'s, and the bending moment showed a 13% increase.

Seismic fragility functions play a vital role in evaluating tunnel vulnerability during both pre- and post-earthquake scenarios [9]. Represented by lognormal fragility curves, these functions provide the probability of a tunnel reaching a certain damage state (*DS*) based on the intensity measure (*IM*) of seismic activity [10]:

$$P[DS \geq \ DS_i |\ IM] \ = \ \Phi\left[\frac{\ln IM - \ln IM_{DS_i}}{\beta_{\text{total}}.DS_i}\right] \tag{1}$$

Table 1: Analytical solutions for calculating lining forces.

Parameter	**Method**	**Slippage condition**	**Mathematical formulation**
Maximum thrust ($T_{\max}$)	Wang [5]	Full slip	$\mathrm{T_{max}} \mp \frac{\mathrm{K_1 E_m}}{6\,(1+\nu_m)} \mathrm{r}\Upsilon_{\max}$
		No slip	$\mathrm{T_{max}} = \mp \mathrm{K_2} \tau_{\max} \mathrm{r} = \mp \frac{\mathrm{K_2 E_m}}{2\,(1+\nu_m)} \mathrm{r}\Upsilon_{\max}$
	Park et al. [7]	Full slip ($D \to \infty$)	$\mathrm{T_{max}} = \mp \frac{(1-\nu_m)\mathrm{E_m r}\Upsilon_{\max}}{(1+\nu_m)\Delta''} \left\{2F + (1-2\nu_m) + 4D \frac{4\mathrm{E_m}}{r\,(1+\nu_m)}\right\}$
		No slip ($D = 0$)	$\mathrm{T_{max}} = \mp \frac{(1-\nu_m)\mathrm{E_m r}\Upsilon_{\max}}{(1+\nu_m)\Delta''} \left\{2F + (1-2\nu_m)C + 4D \frac{4\mathrm{E_m}}{r\,(1+\nu_m)}\right\}$
Maximum bending moment ($M_{\max}$)	Wang [5]	Full slip	$\mathrm{M_{max}} = \mp \frac{1\mathrm{K_1 E_m}}{6\,(1+\nu_m)} \mathrm{r}^2\Upsilon_{\max}$
		No slip	$\mathrm{M_{max}} = \mp \frac{1\mathrm{K_1 E_m}}{6\,(1+\nu_m)} \mathrm{r}^2\Upsilon_{\max}$
	Park et al. [7]	Full slip ($D \to \infty$)	$\mathrm{M_{max}} = \mp \frac{(1-\nu_m)\mathrm{E_m r}^2\Upsilon_{\max}}{(1+\nu_m)\Delta''} \left\{2 + (1-2\nu_m)C + D \frac{4\mathrm{E_m}}{r\,(1+\nu_m)}\right\}$
		No slip ($D = 0$)	$\mathrm{M_{max}} = \mp \frac{(1-\nu_m)\mathrm{E_m r}^2\Upsilon_{\max}}{(1+\nu_m)\Delta''} \left\{2 + (1-2\nu_m)C + D \frac{4\mathrm{E_m}}{r\,(1+\nu_m)}\right\}$

Note: $T_{\max}$ = maximum thrust, E_m = modulus of elasticity of soil or rock medium, r = radius of circular tunnel, $\Upsilon_{\max}$ = maximum free-field shear strain of soil or rock medium, ν_m = Poisson's ratio of soil or rock medium, K_1 = Full-slip lining response coefficient, K_2 = No-slip lining response coefficient, $\tau_{\max}$ = Maximum shear stress, F = flexibility ratio, D = spring-type flexibility coefficient, Δ'' = lining deformation, C = compressibility ratio of tunnel lining and $\mathrm{M_{max}}$ = maximum bending moment.

Eqn (1) involves median threshold IM values and the total lognormal standard deviation (β_{Total}), which is influenced by factors like tunnel support capacity (β_C), seismic demand (β_D), and damage thresholds (β_{DS}):

$$\beta_{\text{total}} = \sqrt{{\beta_C}^2 + {\beta_D}^2 + {\beta_{DS}}^2} \tag{2}$$

This study uses peak ground acceleration (PGA) as the IM, categorizing damage into five distinct levels, from no damage to complete collapse. For RP = 250 year, damage probability reached nearly 100% at a PGA of approximately 0.6 g, as shown in Fig. 2. In contrast,

Table 2: Seismic analysis of Tunnel AST2.

Section		**Chainage (m)**	**Maximum thrust (kN)**		**Maximum bending moment (kN × m)**	
			Wang [5]	**Park et al. [7]**	**Wang [5]**	**Park et al. [7]**
AST2A	2A.1	+000.00 to +125.35	64.35	46.27	182.32	141.53
	2A.2	+125.36 to +248.52	53.23	41.54	75.33	64.09
AST2B	2B.1	+248.52 to +393.12	43.11	35.25	94.32	73.23
	2B.2	+393.13 to +551.74	19.04	16.41	62.43	53.21
	2B.3	+551.75 to +949.26	82.31	64.72	163.21	132.45
AST2C	2C.1	+949.27 to +1,241.38	145.94	123.61	191.03	163.11
	2C.2	+1,241.39 to +1,242.58	157.46	143.05	209.35	185.02

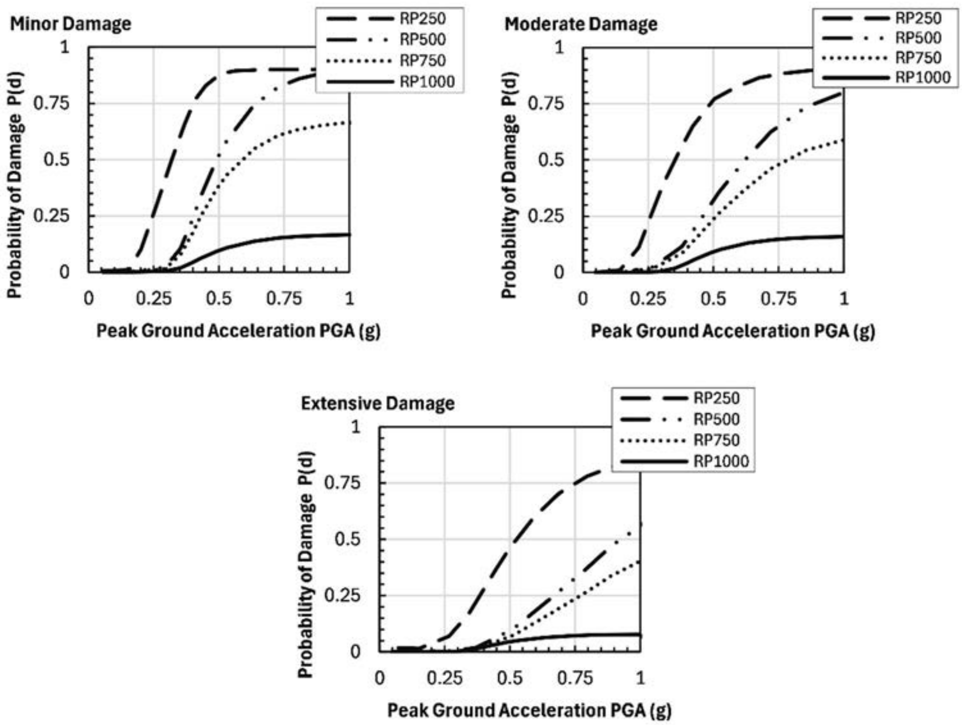

Figure 2: Fragility curves for minor, moderate, and extensive damage cases. RP = return period.

RP = 1,000 year showed a slower increase, requiring a PGA of about 0.75 g to achieve a similar probability of around 50%. Moderate damage exhibited a more pronounced distinction among return periods. RP = 250 year and RP = 500 year indicated rapid escalations in damage probability at lower PGA values (around 0.25 g), reaching probabilities of 80% and 40%, respectively. In contrast, RP = 1,000 year necessitated a considerably higher PGA, achieving about 40% probability at 0.5 g, underscoring the importance of the return period in seismic design. The trend for extensive damage is characterized by a steep increase in damage probability at higher PGA levels. Notably, the RP = 250-year curve ascended sharply, presenting a probability of around 30% at 0.25 g, while RP = 500 year and RP = 750 year stabilized around 15% at similar levels. RP = 1,000 year showed a probability of about 10% at 0.5 g.

3 LOSS AND RESILIENCE MODELING

Werner et al. [11] developed a model to estimate seismic losses (I_s) for transportation infrastructure by factoring in both initial construction costs (C_i) and repair costs (C_r). The mean seismic loss (L_m) over different return periods is determined by evaluating the damage states and the probability (α) of damage impacting the structural components. The formula aggregates the repair costs (C_i^k) for each element of the bridge, factoring in the probability of each damage level (α_i), to calculate the total expected seismic loss [12].

$$L_m(PGA, \alpha) = \sum_{i=0}^{i=4} \sum_{k=1}^{k=n} C_i^k \times \alpha_i \tag{3}$$

The plots presented in Fig. 3 illustrate the exceedance probability (P_e) of seismic loss (I_s) for the AST2 tunnel over various lifespans (T = 0, T = 50, T = 75 and T = 100 years) across different return periods (RP = 1,000, RP = 750, RP = 500 and RP = 250 years). At T = 0 year, all return periods started with an exceedance probability of 1 for minimal seismic loss, demonstrating full functionality. As the lifespan increases, the exceedance probability declines more steeply for shorter return periods (e.g., RP = 250 year) compared to longer periods (e.g., RP = 1,000 year), indicating a higher vulnerability to seismic events over time. The probability plots suggested a critical threshold for seismic loss, where functionality drops to zero (seismic loss of 60,000 USD) for all return periods, highlighting the importance of minimizing losses to maintain operational integrity. Over the evaluated lifespans, the patterns demonstrated that with time, the likelihood of exceeding specific loss values increases, necessitating robust risk mitigation strategies to enhance tunnel resilience against seismic hazards.

The bridge functionality function, ranging between 0 and 1, demonstrates boundedness, monotonicity, and continuity. Cassottana et al. [13] provided a mathematical model describing the recovery process, utilizing bridge functionality ($Q[DS_i \mid t]$) and damage probabilities ($P[DS_i \mid \mathrm{PGA}]$) across different damage states. Ayyub [14] introduced a resilience index (R) to assess bridges' ability to recover, using the earthquake occurrence time (t_e) and the recovery duration (t_r). This index helps pinpoint weaknesses and areas for improvement in the aftermath of earthquake-induced damage.

$$Q(t) = \sum_{i=0}^{4} Q[DS_i \mid t] P[DS_i \mid \mathrm{PGA}] \tag{4}$$

$$R = \frac{\int_{t_e}^{t_r} [\sum_{i=0}^{4} Q[DS_i|t] P[DS_i|\mathrm{PGA}]] \, dt}{t_r - t_e} \tag{5}$$

Fig. 4 illustrates the functionality ($Q(t)$) of the AST2 tunnel, demonstrating its performance over diverse recovery durations (t) across distinct lifespans (T = 0, 50, 75, and 100 years) and return periods (RP = 1,000, RP = 750, RP = 500 and RP = 250 years). At T = 0 year, the functionality is equal to 1.0 for all return periods, indicating complete operational capacity immediately following construction.

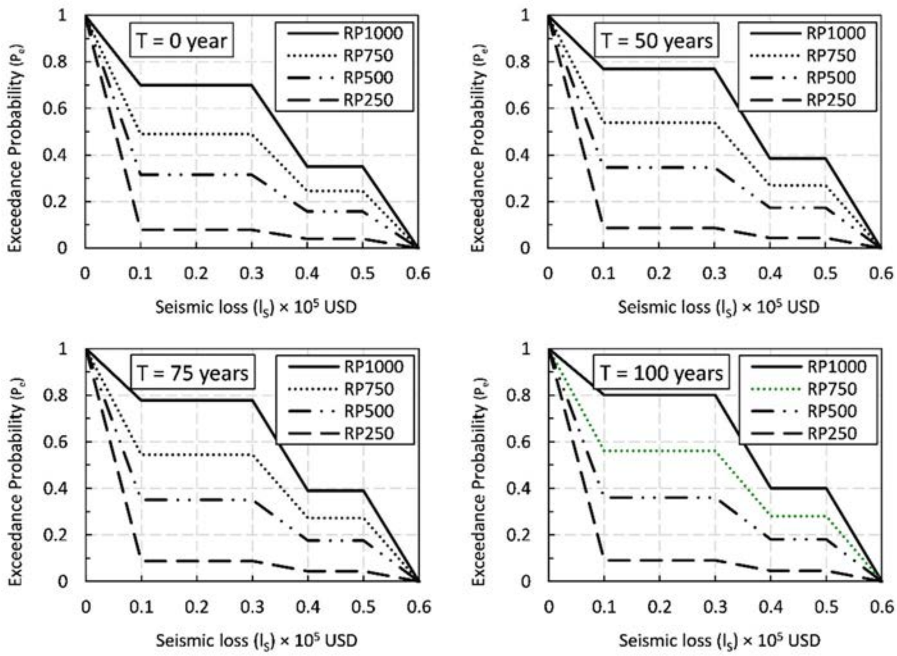

Figure 3: Seismic loss curves across different service lifespans. RP = return period.

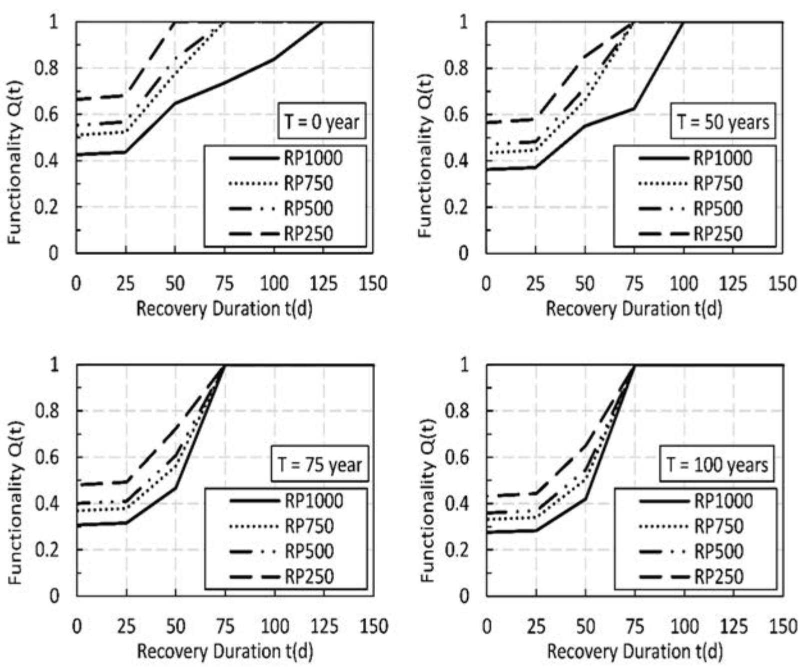

Figure 4: Functionality curves across different service lifespans. RP = return period.

This baseline established the maximum achievable functionality for subsequent evaluations. Recovery trajectories highlighted a distinct relationship between the return period and recovery duration. For T = 0 year, RP = 1,000 year demonstrated rapid initial recovery, achieving functionality levels above 80% within approximately 30 days. In contrast, RP = 250 year exhibited a stagnant recovery, with functionality dropping below 40% even after 150 days, signifying increased sensitivity to more frequent seismic events. As lifespan progressed to T = 100 years, the recovery curves indicated that functionality tends to asymptote at lower levels than those observed in earlier stages. For instance, at T = 100 years, the functionality for RP = 500 year only reached approximately 60%, suggesting a cumulative degradation of structural resilience over time.

4 CONCLUSION AND FUTURE RECOMMENDATIONS

Based on the outcomes of the present study, the following conclusions can be drawn:

- The study highlighted the critical influence of return periods on the probability of various damage levels under peak ground acceleration (PGA), with RP = 250 year indicating a nearly 100% likelihood of minor damage at 0.6 g, while RP = 1,000 year requires significantly higher PGA for similar damage probabilities.
- The percentage variations of maximum thrust and bending moment across various tunnel sections highlighted the differing load demands on these sections, offering critical insights for reinforcing vulnerable zones.
- The trends of seismic loss curves showed the significance of return period selection in seismic design, as shorter return periods lead to quicker reductions in exceedance probability, thereby emphasizing the need for associated resilience planning in the context of seismic risk management.
- The extended timeframes presented in functionality curves revealed that increased exposure to seismic risk over the lifespan correlates with diminished functionality recovery. This decline pattern indicated an inherent vulnerability that accumulates, necessitating a re-evaluation of structural integrity and maintenance protocols.
- The findings suggested implementing rigorous monitoring, maintenance, and retrofitting measures, particularly for tunnels exposed to more frequent seismic activities, to ensure that functionality is preserved or enhanced over the operational lifespan.
- The gradual divergence in functionality recovery indicated the necessity of integrating probabilistic seismic design approaches that account for both the return period and recovery duration in engineering standards, thereby ensuring that the tunnel infrastructure maintains operational integrity under varying seismic scenarios throughout its lifecycle.

The study’s findings offer several practical applications for the sustainable design of tunnels and underground structures, as part of the transportation infrastructure in Oman:

- Targeted reinforcement: Utilize the identified load variations to reinforce specific tunnel sections, enhancing structural resilience while optimizing material usage.
- Seismic design guidelines: Develop design guidelines based on return period insights, ensuring structures are tailored to anticipated seismic risks, thereby enhancing long-term safety and sustainability.
- Proactive maintenance protocols: Implement routine monitoring and maintenance schedules informed by functionality recovery trends, allowing for timely repairs and reducing long-term operational costs.

- Risk-based retrofitting strategies: Establish retrofitting programs for existing tunnels based on their exposure to seismic risks, preserving functionality and extending life.
- Probabilistic design standards: Incorporate probabilistic seismic design approaches into engineering standards, ensuring tunnels can withstand various seismic scenarios and maintain operational integrity over time.

ACKNOWLEDGEMENT

The authors express their gratitude to Sultan Qaboos University (Oman) for providing financial support for this study.

REFERENCES

[1] El-Hussain, I. et al., Probabilistic tsunami hazard assessment along Oman coast from submarine earthquakes in the Makran subduction zone. *Arabian Journal of Geosciences*, **9**, pp. 1–14, 2016.
[2] Ansari, A., El-Hussain, I., Deif, A., Mohamed, A.M., Al-Shijbi, Y., Al-Jabri, K. & Huang, Z., Seismic vulnerability assessment and fragility analysis of tunnels in Oman: Development of risk matrices and functionality guidelines. *Structures*, **69**, 107428, 2024.
[3] St John, C.M. & Zahrah, T.F., Aseismic design of underground structures. *Tunnelling and Underground Space Technology*, **2**(2), pp. 165–197, 1987.
[4] Kouretzis, G.P., Andrianopoulos, K.I., Sloan, S.W. & Carter, J.P., Analysis of circular tunnels due to seismic P-wave propagation, with emphasis on unreinforced concrete liners. *Computers and Geotechnics*, **55**, pp. 187–194, 2014.
[5] Wang, J.N., Seismic design of tunnels: A state-of-the-art approach. Monograph 7, Parsons, Brinckerhoff, Quade and Douglas Inc., New York, 1993.
[6] Penzien, J. ,Seismically induced racking of tunnel linings. *Earthquake Engineering and Structural Dynamics*, **29**(5), pp. 683–691, 2000.
[7] Park, K.H., Tantayopin, K., Tontavanich, B. & Owatsiriwong, A., Analytical solution for seismic-induced ovaling of circular tunnel lining under no-slip interface conditions: A revisit. *Tunnelling and Underground Space Technology*, **24**(2), pp. 231–235, 2009.
[8] Bobet, A., Drained and undrained response of deep tunnels subjected to far-field shear loading. *Tunnelling and Underground Space Technology*, **25**(1), pp. 21–31, 2010.
[9] Ansari, A., Rao, K.S. & Jain, A.K., Seismic response and fragility evaluation of circular tunnels in the Himalayan region: Implications for post-seismic performance of transportation infrastructure projects in Jammu and Kashmir. *Tunnelling and Underground Space Technology*, **137**, pp. 1–13, 2023. https://doi.org/10.1016/j.tust.2023.105118.
[10] Argyroudis, S.A. & Pitilakis, K.D., Seismic fragility curves of shallow tunnels in alluvial deposits. *Soil Dynamics and Earthquake Engineering*, **35**, pp. 1–12, 2012.
[11] Werner, S.D. et al., Redars 2 methodology and software for seismic risk analysis of highway systems (No. MCEER-06-SP08), 2006.
[12] Lee, J.H., Ansari, A., An, H. & Jeong, J.Y., Seismic loss and resilience modelling of bridges in soft soils: Towards design of sustainable transportation infrastructure facilities. *Sustainable and Resilient Infrastructure*, **9**(2), pp. 1–23, 2024. https://doi.org/10.1080/23789689.2024.2328979.
[13] Cassottana, B., Shen, L. & Tang, L.C., Modeling the recovery process: A key dimension of resilience. *Reliability Engineering and System Safety*, **190**, 106528, 2019.
[14] Ayyub, B.M., Systems resilience for multihazard environments: Definition, metrics, and valuation for decision making. *Risk Analysis*, **34**(2), pp. 340–355, 2014.